Features of L-Menthol Crystallization in Optically Active Medium Based on L- and D-Asparaginate Chitosan

Anna B. Shipovskaya*, Natalia O. Gegel, and Xenia M. Shipenok

Department of Polymers, Saratov National Research State University named after N.G. Chernyshevsky, 83 Astrakhanskaya str., Saratov 410012, Russia

*e-mail: shipovskayaab@yandex.ru

Abstract. The phase separation kinetics of an ethanolic L-menthol solution in an aqueous solution of optically and biologically active chitosan L- and D-aspartate was studied. It has been established that this process proceeds according to the extraction crystallization mechanism and combines two types of phase separation, namely: liquid–liquid and liquid–crystal. The effect of aspartic acid stereoisomer, chitosan molecular weight, and polymer: acid ratio on the optical, structural-morphological, and dimensional characteristics of dispersed phase droplets at the initial stage of phase separation and crystal aggregates of the L-menthol condensed phase at the final stage was assessed. In the chitosan D-aspartate medium, as well as with an increase in the concentration of components in the optically active medium and the molecular weight of the polymer, the rate of phase separation, the size of droplets and particles increase. It has been suggested that the system under study is promising for encapsulating hydrophobic drugs, creating chirooptic waveguides, and sensors for biomedical purposes, as well as developing new methods for studying the fundamental principles of phase separation in intracellular regulation of membraneless organelles and subcellular organization of biosystems, including under stress conditions of a living organism underlying the development of new pharmaceuticals to treat rare and currently incurable diseases. © 2023 Journal of Biomedical Photonics & Engineering.

Keywords: chitosan; L- and D-aspartic acid; salt formation; L-menthol; phase separation; extraction crystallization; spherulites; intracellular regulation; subcellular organization.

1 Introduction

Achieving control over the molecular and structural chirality of the created product is one of the urgent problems of modern materials science in the field of stereospecific polymeric materials for biomedical purposes. This is primarily due to some functional features of such systems, which provide fundamentally novel chirooptic and complementary-selective properties inaccessible for achiral polymeric materials [1–4]. For example, salt complexes of the aminopolysaccharide chitosan (CS) with L- and D-ascorbic acid (AscA) or L- and D-aspartic acid (AspA) significantly differ in chirooptic, structural-morphological, and biological properties from traditional chitosan-containing materials obtained from polymer solutions in optically inactive carboxylic acids, depending on the stereoisomer (L- or D-) of the acid used [5−7]. At the same time, CS salts with the biologically inactive D-isomers of AscA and AspA have the best properties, while the L-isomer of AscA (vitamin C) or AspA (an essential amino acid) exhibits the highest biological activity in the case of individual acids.

The specific biological role of D-isomers of the acids is no longer considered as a rare occurrence, since recent studies have revealed a deviation from the previously

declared "chiral purity" of biosystems, in particular, the principle of constructing natural proteins from L-amino acids only. It has turned out that, in addition to the detection of D-amino acids in the cell walls of prokaryotes, free D-amino acids are involved in normal metabolism and in the regulation of eukaryotic vital activity [8]. D-AspA has been found in mammalian hormone-producing cells [9] and human dental dentin [10]. It has also been established that it is not the natural biologically active L-isomer which is effective in the treatment of certain diseases, but its synthetic D-antipode [11, 12]. In addition, D-amino acids have been shown to be highly effective in destroying biofilms and reducing the antibiotic resistance of living organisms, which has opened up new directions for the development of personalized antimicrobial drugs [13, 14].

One of the informative approaches to assessing the stereospecificity of the spatial organization of L- and D-isomer chitosan salts can be considered the study of their interaction with some chiral, optically pure and, at the same time, biologically active compound, e.g., L-menthol. This organic substance belongs to the class of cyclic monoterpene alcohols, it is solid at room temperature and melts within 42–45 °C (α-phase), is insoluble in water and readily soluble in ethyl alcohol, chloroform and acetone, has optical activity (in solution) and optical anisotropy (in melts). Depending on the conditions of phase separation (temperature gradient, cooling rate, substrate structure, solvent, and precipitating medium), it is characterized by a variety of morphostructures formed in this process. For example, ring-shaped spherulites are formed during thermally induced crystallization from a melt in an air atmosphere, in which acicular crystals (whiskers) of L-menthol self-organize into radially oriented periodic regions with high and low densities of the solid phase of the substance, or non-banded continuous spherulites, consisting of densely packed lamellar crystals [15]. Such rhythmic crystallization could be due to the chirality of L-menthol [16], as well as nonlinear diffusion of the substance during mass transfer [17, 18] and the "unbalanced" surface energy of the system [19]. During thermally induced crystallization in an aqueous medium (antisolvent), the phase transition from the liquid–liquid region to the solid–liquid one is accompanied by the formation of the stable α-polymorphic form of L-menthol [20, 21]. When dispersing an L-menthol solution in ethanol or chloroform into an aqueous medium, a phase separation of the liquid–liquid type is observed with the formation of an oil-in-water emulsion, whose dispersed phase is represented by nano- and microscopic drops of the hydrophobic component [22−24]. The liquid–liquid type of phase separation was successfully used for the encapsulation of L-menthol into nano- and microcapsules made of chitosan (solutions in CH_3COOH and additional cross-linking of the polymer with Na tripolyphosphate) [25], the vegetable protein zein [23], or polycaprolactone [24] were used, and specific thermally induced crystallization

with no use of any organic solvent was successfully used for the encapsulation of L-menthol into monodisperse spherical micro- and macroparticles [20], thus ensuring stabilization, controlled delivery and release of this substance. The use of L-menthol as an initiator of multiepitaxial oriented crystallization (liquid-phase epitaxy) made it possible to obtain ordered and aligned poly-lactic-co-glycolic acid nanofibers for tissue engineering scaffolds and neural interface systems [22].

L-menthol has low toxicity for humans [26, 27]. In addition to well-known cooling properties and a characteristic minty odor, L-menthol exhibits anesthetic, antibacterial, antitumor and immunomodulatory effects, and is also an effective agent for transdermal drug transport [22, 28]. It has also demonstrated the ability to act as an inhibitory molecule on voltage-gated channels which significantly affect the neurotransmission functions of a living organism and gene expression in various cell types [29]. Based on the above properties and taking into account the molecular chirality and variety of supramolecular chiral symmetries formed under varying crystallization conditions, L-menthol can be considered as a model biosystem for studying the stereospecificity of the chiral polymeric materials developed. In particular, we considered L-menthol to be suitable for studying the decay kinetics of optical anisotropy intensity during phase separation of this substance in a chiral aqueous medium based on the optically and biologically active chitosan L- and D-aspartate. This process mimics liquid-phase separation during intracellular signal transduction [30, 31].

We have previously found that the interaction of an aqueous solution of chitosan ascorbate and an L-menthol solution in ethyl alcohol or its mixture with acetone is accompanied by crystalline phase separation of the mixture system to form anisodiametric fibrillar entities in the case of CS in L-AscA, which exhibit pronounced optical anisotropy in polarized light, or densely packed confocal domains of a shape close to spherical in the case of CS in D-AscA [5, 6]. In this work, we will consider features of the crystallization of the L-menthol + ethanol system in an aqueous solution of CS in L- and D-AspA.

2 Materials and Methods

The following reagents were used: chitosan hydrochloride with a viscosity average molecular weight $\overline{M}_\eta = 38$ kDa (CS-38), a degree of deacetylation DD = 80 mol %, and chitosan with $\overline{M}_\eta = 200$ kDa (CS-200), DD = 82 mol % (Bioprogress Ltd., RF); L-AspA (JSC Bioamid, RF); D-AspA (Vekton Ltd., RF); L-menthol with a 99% basic substance (Alfa Aesar, Heysham, Lancs, UK); 95% ethyl alcohol (RFK Corp., Orel, RF); and distilled water. All reagents were chemical grade and used without further purification.

To prepare solutions of chitosan L- and D-asparaginate, weighed portions of CS, L- and D-AspA powders were dissolved in distilled water under stirring on a magnetic stirrer at 50 °C for 3 h. The concentration

A.B. Shipovskaya et al.: Features of L-Menthol Crystallization in...

doi: 10.18287/JBPE23.09.010305

of CS was varied in the range of 0.3–0.8 g/dL, those of L- and D-AspA were varied within 0.2–0.6 g/dL. Since the protonation degree of $-NH_2$ groups of CS upon its dissolution in an aqueous AspA solution does not exceed 0.8–0.9 [32], the molar ratio [AspA]/[$\sim$-NH_2] = 0.85−0.95 mol/monomol was observed in the preparation of solutions to eliminate the influence of unbound acid. A solution of L-menthol with a concentration of 2.5 g/dL was prepared by dissolving a sample of air-dry L-menthol in 95% ethyl alcohol for 24 h.

Surface tension was measured on a K20 automatic tensiometer (KRÜSS GmbH, Germany) using the Wilhelmy plate method at 25 °C.

To explore the kinetics of phase separation, 3 ml of an aqueous solution of CS in L-(D-)AspA was poured into a Petri dish 3 cm in diameter, and 1.5 ml of an ethanolic L-menthol solution was added dropwise onto the surface of the liquid medium with an automatic dispenser without stirring the system. The Petri dish was covered with a cover slip and left under static conditions in an air atmosphere at a temperature of 22 ± 2 ºC for 24 h. The phase separation process was considered complete if there were no changes in both the size and morphostructure of the condensed phase and the disappearance of any birefringence effect.

The kinetics of phase separation was observed both visually and on a LaboPol-2 (RF) polarization microscope (PM) with the polarizer and analyzer crossed. A halogen lamp (12 V, 30 W) served as the light source. PM-photos were obtained by a DMC 300 (3 Mpx) USB camera (Hangzhou, China). The size of the forming phases (droplets and solid-phase particles) was measured using the scale of an eyepiece micrometer with a division value of 0.01 mm. The effective diameter was taken as the size of droplets and particles with shapes close to spherical, while the largest characteristic effective diameter (largest transverse size) was taken as the size of particles with a noticeably different from spherical shape.

The morphology of the air-dry condensed phase of L-menthol isolated at the final stage of phase separation was evaluated by scanning electron microscopy (SEM) on a MIRA\\LMU scanning electron microscope (Czech Republic) at a voltage of 15 kV and a conductive current of 400 pA. The sample preparation was carried out as follows: the liquid phase was removed from the Petri dish with a plastic pipette, the remaining condensed phase was dried in air at 22 ± 2ºC for 24 h until the formation of an air-dry state of the substance, then the resulting object was fixed on a standard aluminum table of an electronic microscope with plastic tweezers and deposited a gold layer 5 nm thick using a K450X Carbon Coater (Germany).
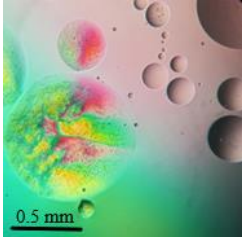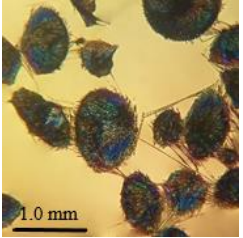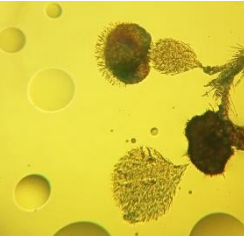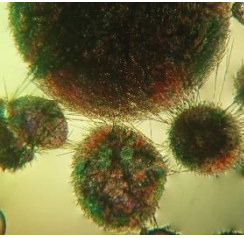
3 Results and Discussion
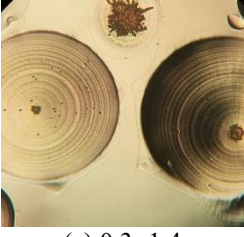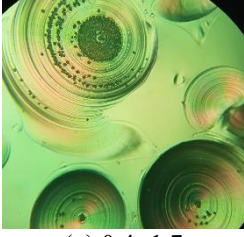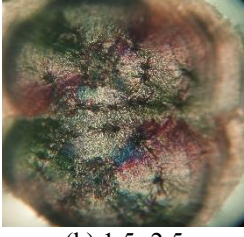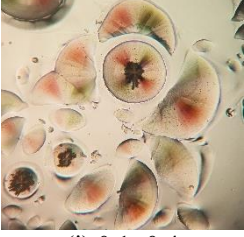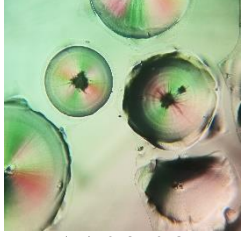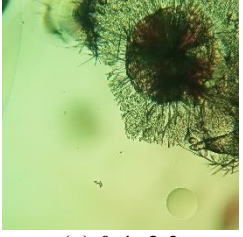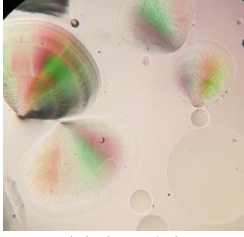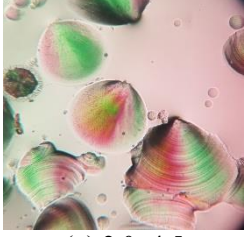
Studying L-menthol crystallization in an optically active aqueous medium, we discovered a new feature of the phase separation of this substance (not having noted by other authors), which consists in a combination of two types of phase separation, namely: liquid–liquid and liquid–crystal. After applying the ethanolic L-menthol solution to the surface of the aqueous solution of CS L- and D-aspartate, the spontaneous dispersion of the hydrophobic weakly polar component in the aqueous medium begins almost immediately to form a direct oil-in-water microemulsion. The liquid–liquid phase separation proceeds very intensively and visually resembles the process of water seething, just without a characteristic sound background. Subsequently, the process of coalescence of microdroplets proceeds, and crystallization of the optically active low-molecular-weight substance proceeds in the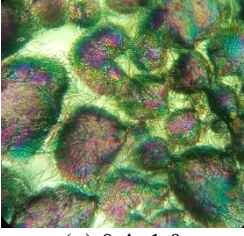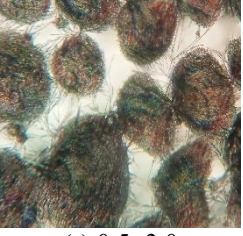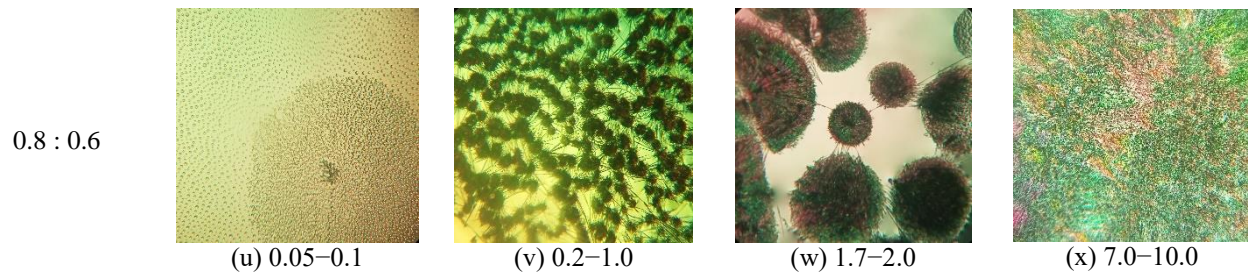 macrodroplets of the dispersed phase. Table 1 gives PM-photos and the size of droplets and particles formed during the phase separation of L-menthol in the solutions of CS-38(-200) in L- and D-AspA.

Consider the kinetics of the phase formation process of the L-menthol + ethanol system in an aqueous solution of chitosan L- and D-aspartate. At the initial stage of phase separation (2–5 min after the start of the experiment), drops of the alcoholic menthol solution, which have microscopic dimensions and are initially isotropic, increase up to millimeter sizes due to Brownian aggregation of particles and acquire birefringence. When observed in a polarizing optical microscope through a system of crossed polarizers, it is clearly seen that phase-separated optically anisotropic macrodroplets of the oil phase are characterized by a ring ordering of the substance with a radial orientation of multi-colored texture patterns (anisotropic periodic spherulites), Maltese-cross textures are also observed, which indicates the beginning of L-menthol crystallization. With an increase in the concentration of CS : AspA components in the antisolvent liquid phase, the phase formation rate increases, and the droplet size decreases, which may be due to the superposition of the effects of increased viscosity of the polymer solution with a simultaneous decrease in the protonation degree of its $-NH_2$ groups [32].

At the next stage of the phase separation of the system (5–30 min), the macrodroplets of the dispersed phase (hydrophobic in nature) are separated from the dispersion medium (not only by PM, but also visually) and L-menthol crystallization continues therein to form spherical or ovoid solids particles of non-banded spherulite morphology, consisting of densely packed whiskers. In some cases, coalescence of such particles and individual whiskers into larger supramolecular formations is observed (see photo (r), (t), and (v) in Table 1) and even their coalescence into a continuous optically anisotropic crystalline phase (photo (x) in Table 1). In this case, birefringence attenuation is observed, and the effect of optical anisotropy disappears after 24 h, which is expressed in the disappearance of the color effect of the glow of objects. The molecular weight of CS has little effect on the morphostructure of liquid-like oily droplets and aggregates of L-menthol whiskers, but its increase raises the phase separation rate, the density and thickness of the condensed phase.

Table 1 PM photos of the extraction crystallization stages of an ethanolic L-menthol solution in aqueous CS solutions in L- and D-AspA with varying concentrations of CS : AspA, magnification ×40. The range of effective diameter (min−max) of droplets and particles formed is indicated under the photos.

Concentration CS : AspA (g/dL : g/dL)	PM-photos and droplet/particle size (mm)			
	CS · L-AspA		CS · D-AspA	
	Extraction crystallization time (min)			
	5	30	5	30
CS-38				
0.3 : 0.2	(a) 0.1−0.7	(b) 1.0−1.4	(c) 0.2−0.7	(d) 1.3−1.8
0.6 : 0.4	(e) 0.3−1.4	(f) 1.2−1.4	(g) 0.4−1.7	(h) 1.5−2.5
0.8 : 0.6	(i) 0.1−0.4	(j) 0.2−0.8	(k) 0.3−0.8	(l) 0.5−1.3
CS-200				
0.3 : 0.2	(m) 0.3−0.8	(n) 0.4−2.3	(o) 0.5−1.0	(p) 2.0−4.5
0.6 : 0.4	(q) 0.4−1.0	(r) 0.5−3.0	(s) 2.0−4.5	(t) 3.0−7.0

0.8 : 0.6

(u) 0.05−0.1   (v) 0.2−1.0   (w) 1.7−2.0   (x) 7.0−10.0

According to the phase diagram [23], intensive dispersion of the ethanolic L-menthol solution in the achiral aqueous medium results in liquid phase separation to form an emulsion. Suspended emulsion drops are unstable; they spontaneously coalesce over time due to the system tending to a minimum of its free energy by decreasing the phase interface, which leads to the separation of the system into two liquid macrophases. In the case of dispersion of the ethanolic L-menthol solution in the chiral aqueous medium based on CS in L- and D-AscA, solid-phase separation was fixed with the precipitation of mixed polymorphic crystalline CS-menthol modifications [5, 6]. Based on the above, the phase separation of L-menthol in the chiral aqueous medium based on CS in L- and D-AspA, combining spontaneous liquid-phase (in the absence of convection and mixing) and solid-phase (in the absence of a temperature gradient) phase separation, is essentially selective extraction crystallization of the chiral low-molecular-weight substance: it was observed for the first time for the objects studied. This process is probably due to a significant difference in the surface energy of the achiral and chiral aqueous media. For example, the surface tension of H_2O at 25 ºC is 71.9 mN/m, while that of CS solutions in L- and D-AspA at CS : AspA = 0.8 : 0.6 g/dL : g/dL are 47.1 and 43.4 mN/m, respectively.

It should also be noted the influence of the AspA isomer on the formation rate of L-menthol micro- and macroemulsions, as well as the size characteristics of the droplets and particles formed. In the aqueous CS · D-AspA-based medium, the rate of liquid–liquid and liquid–solid phase separation is significantly higher than in that on the basis of CS · L-AspA. The size of the oily phase droplets and anisotropic crystalline particles is also significantly higher during phase formation in the CS · D-AspA medium. In the CS ·L-AspA solution, the crystallites of the dispersed phase almost do not aggregate, forming only dendritic entities of non-banded spherulites and primary structural elements (filamentous whiskers), while in the CS · D-AspA medium (especially at high concentrations of CS : AspA), the whiskers coalesce into a compacted condensed phase, which is confirmed by SEM.

As an example, Fig. 1 shows SEM photos of the air-dry condensed phase isolated during the extraction crystallization of L-menthol in the aqueous solution of CS-200 in L- and D-AspA at the component concentration of 0.6 : 0.4 g/dL : g/dL.
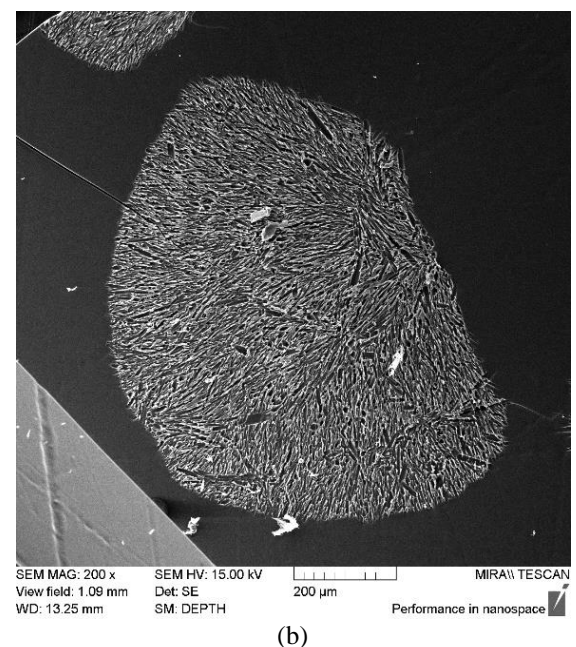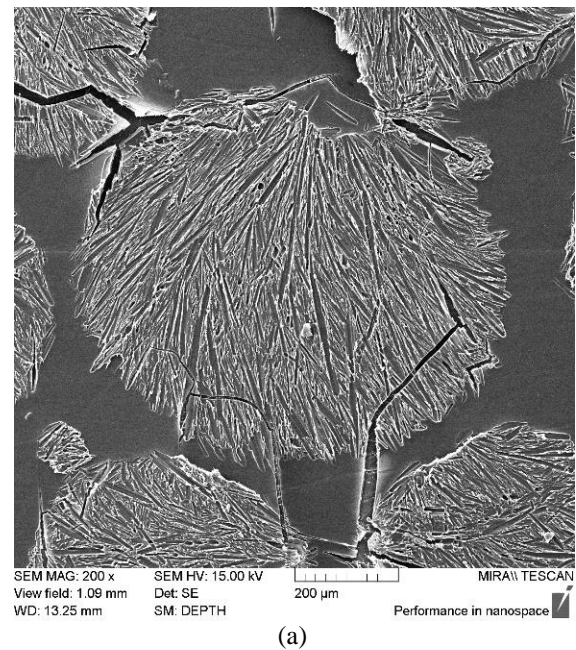

(a)

(b)

Fig. 1 SEM photos of the condensed phase isolated during the extraction crystallization of the ethanolic L-menthol solution in the aqueous CS-200 solution in L-AspA (a) and in D-AspA (b) at the concentration of components CS-200 : L-(D-)AspA = 0.6 : 0.4 g/dL : g/dL; the scale mark, 200 µm.

For ease of comparison, non-banded spherulites of similar size were selected. Darker and lighter whiskers correspond to high-density and low-density crystalline packing, respectively, while extended dark bands, matching the background color of the SEM photo, correspond to an empty area (no crystals). As can be seen, the crystallites are represented by the so-called leaky radial configuration, when whiskers grow from one point into a cone-shaped space and the angle between the main axes of the growing whiskers is approximately 20−30º. At the same time, the condensed L-menthol phase obtained in the CS-200 · L-AspA medium is more loose than that obtained in the CS-200 · D-AspA medium.

We should also dwell on the difference in orientational ordering and supramolecular chirality of non-banded crystal structures obtained in this work in an optically active aqueous medium and in an achiral aqueous medium in Ref. [15]. Non-banded L-menthol spherulites during thermally induced phase separation (in the absence of a liquid medium) are formed due to the spatial growth of lamellar crystals or of whiskers during extraction crystallization in a chiral aqueous medium. Lamellar spherulites have a twist-radial orientation, i.e. spherical symmetry about the center, since the crystals grow radially from a common center in the disk space and twist along the radius of the spherulite. Acicular spherulites of leaked radial orientation have no center of symmetry due to the radial growth of crystals from a common point in a conical space. Thus, acicular spherulites, in addition to molecular chirality, exhibit macroscopic chirality as well.

4 Conclusion

We have studied the decay kinetics of the intensity of the optical anisotropy of the L-menthol + ethanol system at a qualitative level during its phase separation in an aqueous solution of L- and D-chitosan aspartate. We emphasize once again that this process proceeds spontaneously according to the extraction crystallization mechanism and combines two types of phase separation, namely:

liquid–liquid and liquid–crystal. The effect of AspA stereoisomer, variation of the CS : L-(D-)AspA ratio, and polymer molecular weight on the optical anisotropy, morphostructure, and droplet size of the dispersed phase at the initial stage of phase separation and phase aggregates of the L-menthol crystalline phase at the final stage was assessed. It has been established that in the CS · D-AspA medium, in contrast to CS · L-AspA, larger particles of oily droplets and aggregated L-menthol crystals are formed, which coalesce in time into a continuous optically anisotropic condensed phase. With an increase in the CS : L-(D-)AspA concentration and the molecular weight of the polymer, the rate of phase separation increases.

The results obtained open up extremely interesting practical applications. It is expected that aqueous CS solutions in L- or D-AspA can be used to encapsulate not only L-menthol, but also other hydrophobic drugs into microcapsules and microparticles, as well as to design new types of chirooptic waveguides and biomedical sensors. In addition, since biochemical reactions inside cells proceed in the limited spaces of both classical membrane and non-membrane organelles (cell bodies in the form of a liquid drop formed as a result of the liquid–liquid phase separation [30, 31]), the hydroalcoholic CS · L-(D-)AspA + L-menthol system could be very useful for studying the fundamental principles of intracellular communication and regulation in both physiological and pathological cellular processes.

Disclosures

All authors declare that there is no conflict of interests in this paper.

Acknowledgements

References

1. M. Mabrouk, S. F. Hammad, A. A. Abdella, and F. R. Mansour, "Enantioselective chitosan-based racemic ketoprofen imprinted polymer: chiral recognition and resolution studym," International Journal of Biological Macromolecules 200, 327–334 (2022).
2. C. Liu, C. Dong, S. Liu, Y. Yang, and Z. Zhang, "Multiple chiroptical switches and logic circuit based on salicyl-imine-chitosan hydrogel," Carbohydrate Polymers 257, 117534 (2021).
3. X. Dou, N. Mehwish, C. Zhao, J. Liu, C. Xing, and C. Feng, "Supramolecular hydrogels with tunable chirality for promising biomedical applications," Accounts of Chemical Research 53(4), 852–862 (2020).
4. L. Xu, Y. A. Huang, Q. J. Zhu, and C. Ye, "Chitosan in molecularly-imprinted polymers: Current and future prospects," International Journal of Molecular Sciences 16(8), 18328–18347 (2015).
5. A. B. Shipovskaya, O. N. Malinkina, N. O. Gegel, I. V. Zudina, and T. N. Lugovitskaya, "Structure and properties of chitosan salt complexes with ascorbic acid diastereomers," Russian Chemical Bulletin 70(9), 1765–1774 (2021).
6. N. O. Gegel, Yu. Yu. Zhuravleva, A. B. Shipovskaya, O. N. Malinkina, and I. V. Zudina, "Influence of chitosan ascorbate chirality on the gelation kinetics and properties of silicon-chitosan-containing glycerohydrogels," Polymers 10(3), 259–275 (2018).

7. A. B. Shipovskaya, N. O. Gegel, X. M. Shipenok, O. S. Ushakova, T. N. Lugovitskaya, and I. V. Zudina, "Structure, properties and biological activity of chitosan salts with L- and D-aspartic acid," Biology and Life Sciences Forum 20(1), 5 (2022).

8. V. A. Tverdislov, L. V. Yakovenko, and A. A. Zhavoronkov, "Chirality as a problem of biochemical physics," Russian Chemical Journal LI(1), 13–22 (2007) [in Russian].

9. A. D'Aniello, "D-aspartic acid: an endogenous amino acid with an important neuroendocrine role," Brain Research Reviews 53(2), 215234 (2007).

10. S. C. Zapico, D. H. Ubelaker, and J. Adserias-Garriga, "Applications of physiological bases of aging to forensic science," Chapter 13 in Forensic Science and Humanitarian Action: Interacting with the Dead and the Living, R. C. Parra, S. C. Zapico, and D. H. Ubelaker (Eds.), John Wiley & Sons Ltd., New York, 183-197 (2020).

11. J. Patočka, Z. Navrátilová, "D-serin: Od kuriózní molekuly k potenciálnímu psychofarmaku [D-serine: from curiosity molecule to potential psychopharmaceutical]," Psychiatry 23(3), 142–147 (2019).

12. A. González-Sarrías, M. Á. Núñez-Sánchez, R. García-Villalba, F. A. Tomás-Barberán, and J. C. Espín, "Antiproliferative activity of the ellagic acid-derived gut microbiota isourolithin A and comparison with its urolithin A isomer: the role of cell metabolism," European Journal of Nutrition 56(2), 831–841 (2017).

13. E. Adaligil, K. Patil, M. Rodenstein, and K. Kumar, "Discovery of peptide antibiotics composed of D-amino acids," ACS Chemical Biology 14(7), 1498–1506 (2019).

14. R. Kumar, N. Singh, A. Chauhan, M. Kumar, R. S. Bhatta, and S. K. Singh, "Mycobacterium tuberculosis survival and biofilm formation studies: effect of D-amino acids, D-cycloserine and its components," Journal of Antibiotics 75, 472–479 (2022).

15. T. Kovács, R. Szűcs, G. Holló, Z. Zuba, J. Molnár, H. K. Christenson, and I. Lagzi, "Self-assembly of chiral menthol molecules from a liquid film into ring-banded spherulites," Crystal Growth & Design 19(7), 4063–4069 (2019).

16. A. G. Shtukenberg, Y. O. Punin, A. Gujral, and B. Kahr, "Growth actuated bending and twisting of single crystals," Angewandte Chemie International Edition 53(3), 672−699 (2014).

17. H.-F. Wang, C.-H. Chiang, W.-C. Hsu, T. Wen, W.-T. Chuang, B. Lotz, M.-C. Li, and R.-M. Ho, "Handedness of twisted lamella in banded spherulite of chiral polylactides and their blends," Macromolecules 50, 5466−5475 (2017).

18. T. Kyu, H. W. Chiu, A. J. Guenthner, Y. Okabe, H. Saito, and T. Inoue, "Rhythmic growth of target and spiral spherulites of crystalline polymer blends," Physical Review Letters 83(14), 2749−2752 (1999).

19. J. Xu, H. S. Ye, Zhang, and B. Guo, "Organization of twisting lamellar crystals in birefringent banded polymer spherulites: a mini-review," Crystals 7(8), 241–251 (2017).

20. M. Sun, S. Du, W. Tang, L. Jia, and J. Gong, "Design of spherical crystallization for drugs based on thermal-induced liquid-liquid phase separation: case studies of water-insoluble drugs," Industrial & Engineering Chemistry Research 58(44), 20401–20411 (2019).

21. I. De Albuquerque, M. Mazzotti, "Influence of liquid-liquid phase separation on the crystallization of L-Menthol from water," Chemical Engineering & Technology 40(7), 1339–1346 (2017).

22. E. Betz-Güttner, M. Righi, S. Micera, and A. Fraleoni-Morgera, "Directional growth of cm-long PLGA nanofibers by a simple and fast wet-processing method," Materials 15(2), 687 (2022).

23. S. Kim, S. C. Peterson, "Optimal conditions for the encapsulation of menthol into zein nanoparticles," LWT 144, 111213 (2021).

24. A. Ferri, N. Kumari, R. Peila, and A. A. Barresi, "Production of menthol-loaded nanoparticles by solvent displacement," Canadian Journal of Chemical Engineering 95(9), 1690–1706 (2017).

25. R. Nuisin, J. Krongsin, S. Noppakundilograt, and S. Kiatkamjornwong, "Microencapsulation of menthol by crosslinked chitosan via porous glass membrane emulsification technique and their controlled release properties," Journal of Microencapsulation 30(5), 498–509 (2013).

26. A. M. Api, D. Belsito, D. Botelho, D. Browne, M. Bruze, G.A. Burton Jr., J. Buschmann, M.L. Dagli, M. Date, W. Dekant, C. Deodhar, M. Francis, A.D. Fryer, K. Joshi, S. La Cava, A. Lapczynski, D.C. Liebler, D. O'Brien, R. Parakhia, A. Patel, T. M. Penning, G. Ritacco, J. Romine, D. Salvito, T. W. Schultz, I. G. Sipes, Y. Thakkar, E. H. Theophilus, A. K. Tiethof, Y. Tokura, S. Tsang, and J. Wahler, "RIFM fragrance ingredient safety assessment, menthyl isovalerate CAS registry number 16409-46-4," Food and Chemical Toxicology 110, S486–S495 (2017).

27. H. K. Vaddi, P. C. Ho, Y. W. Chan, and S. Y. Chan, "Terpenes in ethanol: haloperidol permeation and partition through human skin and stratum corneum changes," Journal of Controlled Release 81(1–2), 121–133 (2002).

28. G. P. P. Kamatou, I. Vermaak, A. M. Viljoen, and B. M. Lawrence, "Menthol: a simple monoterpene with remarkable biological properties," Phytochemistry 96, 15–25 (2013).

29. M. Oz, E. G. El Nebrisi, K. H. S. Yang, F. C. Howarth, and L. T. Al Kury, "Cellular and molecular targets of menthol actions," Frontiers in Pharmacology 8, 472 (2017).

30. S. V. Nesterov, N. S. Ilyinsky, and V. N. Uversky, "Liquid-liquid phase separation as a common organizing principle of intracellular space and biomembranes providing dynamic adaptive responses," Biochimica et Biophysica Acta – Molecular Cell Research 1868(11), 119102 (2021).

31. D. M. Mitrea, R. W. Kriwacki, "Phase separation in biology; functional organization of a higher order," Cell Communication and Signaling 14, 1 (2016).

32. T. N. Lugovitskaya, A. B. Shipovskaya, S. L. Shmakov, and X. M. Shipenok, "Formation, structure, properties of chitosan aspartate and metastable state of its solutions for obtaining nanoparticles," Carbohydrate Polymers 277, 118773 (2022).